Supplementary Information

Table of Contents:

16. Figure SI-13: Average chloride coordination number per zinc as a function of total chloride concentration for pure and mixed salt solutions derived from various theoretical and experimental methods.
17. Figure SI-14: TDDFT calculated VTC-XES spectra for dimer $Zn_2Cl_3^-$ and monomer $ZnCl_3^-$.
18. Figure SI-15: VTC-XES spectra for 1 molal $ZnCl_2$ aqueous solutions with added NaCl and LiCl.
19. Details of the N_{Cl} calculation.
20. Ancillary information about the CMD force field.

Table SI-1: DFT optimized structures used for TDDFT calculations with average bond length and standard deviation.

Coordination Complex (Symmetry)	Zn first shell ligand	Bond length (Å)	Standard Deviation (Å)		Coordination Complex (Symmetry)	Zn first shell ligand	Bond length (Å)	Standard Deviation (Å)
$Zn(H_2O)_6^{+2}$ (Octahedral)	O	2.11	0.03		$Zn(H_2O)_6^{+2}$ (Octahedral)	O	2.11	0.03
$ZnCl(H_2O)_3^{+}$ (Tetrahedral)	O	1.97	0.02		$ZnBr(H_2O)_3^{+}$ (Tetrahedral)	O	1.97	0.02
	Cl	2.28	0.00			Br	2.37	0.00
$ZnCl_2(H_2O)_2$ (Tetrahedral)	O	1.96	0.02		$ZnBr_2(H_2O)_2$ (Tetrahedral)	O	1.97	0.00
	Cl	2.30	0.02			Br	2.40	0.02
$ZnCl_3H_2O^{-}$ (Tetrahedral)	O	1.98	0.00		$ZnBr_3H_2O^{-}$ (Tetrahedral)	O	1.98	0.00
	Cl	2.28	0.01			Br	2.40	0.00
$ZnCl_4^{-2}$ (Tetrahedral)	Cl	2.30	0.02		$ZnBr_4^{-2}$ (Tetrahedral)	Br	2.42	0.02

Table SI-2: Zn – Cl coordination numbers for 1 m $ZnCl_2$ with added LiCl extracted from references 53 and 54 in the manuscript.

Zn – Cl Coordination numbers for: 1 m $ZnCl_2$ + (*x*) LiCl			
x	**2.5 m**	**5 m**	**10 m**
Pluharova et al.[53]	2.92	3.08	3.14
Nguyen et al.[54]	2.71	2.80	2.99

Table SI-3: Linear decomposition of intermediate moiety spectra onto the endpoint spectra from TDDFT.

Moiety	**Octahedral contribution**	**Tetrahedral contribution**
$Zn(H_2O)_6^{+2}$	1	0
$ZnCl(H_2O)_3^{+}$	0.55	0.45
$ZnCl_2(H_2O)_2$	0.31	0.69
$ZnCl_3(H_2O)^{-}$	0.16	0.84
$ZnCl_4^{-2}$	0	1

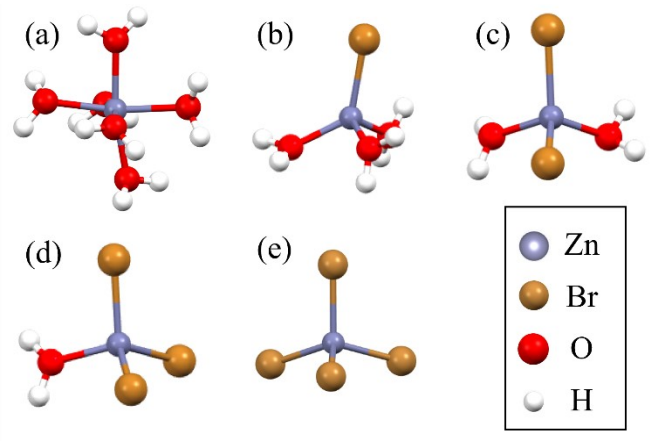

Figure SI-1. DFT optimized structures for Zn^{+2} complex with Br^{-} addition.

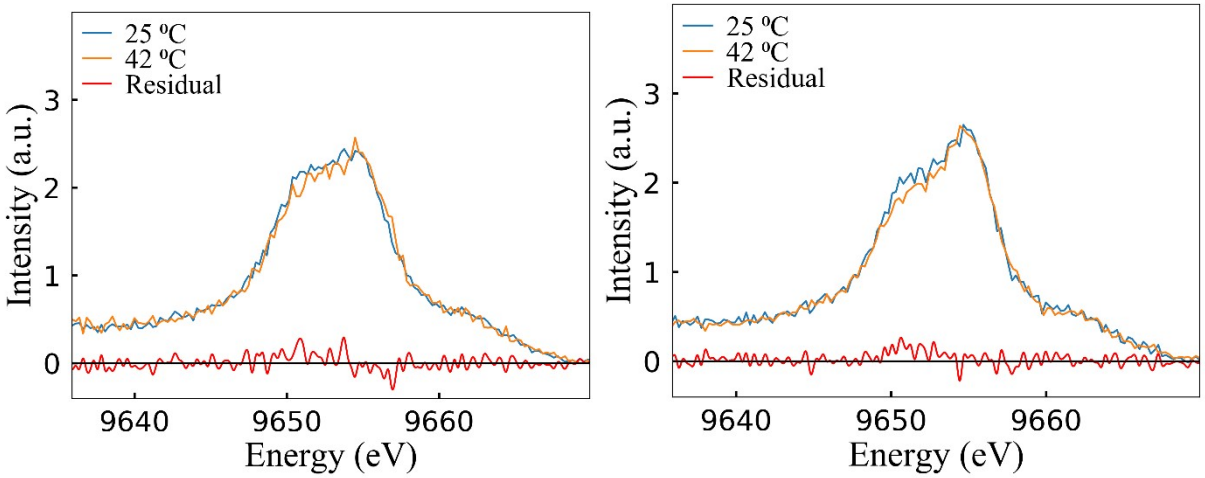

Figure SI-2: VTC-XES spectra at 25°C and 42°C for (a) 1 m ZnCl2 + 0.5 m NaCl and (b) 1 m ZnCl2 + 1 m NaCl, showing the small difference within permissible error (4% octahedral contribution change was noticed in the LCA).

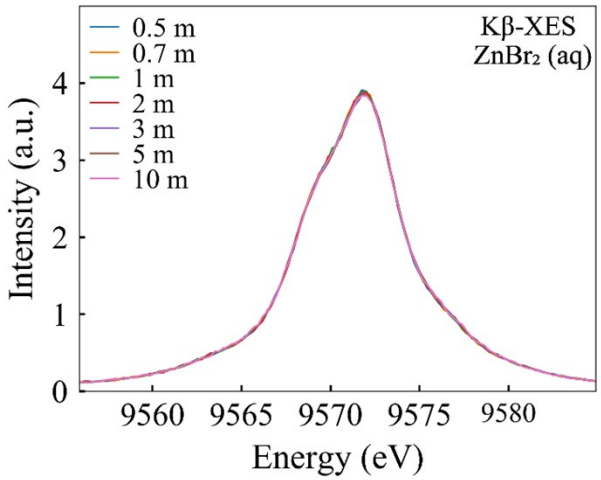

Figure SI-3: Representative Zn Kβ XES spectra for aqueous $ZnBr_2$ concentration series showing excellent alignment after normalization.

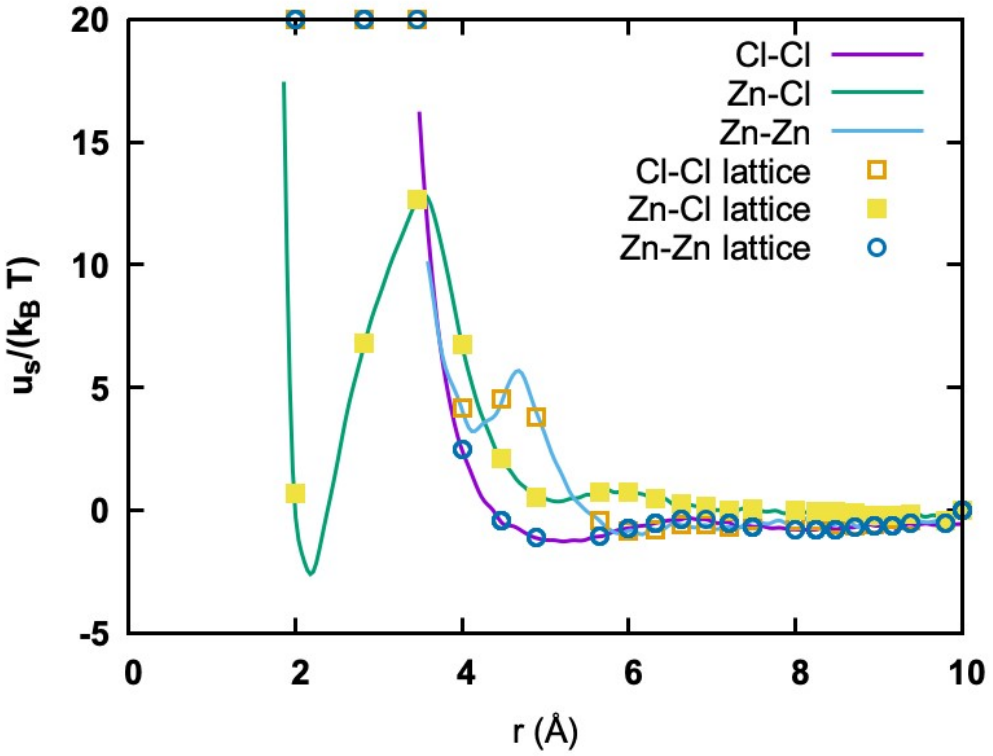

Figure SI-4: Short range potential and location of lattice interaction distances used for Monte Carlo simulations.

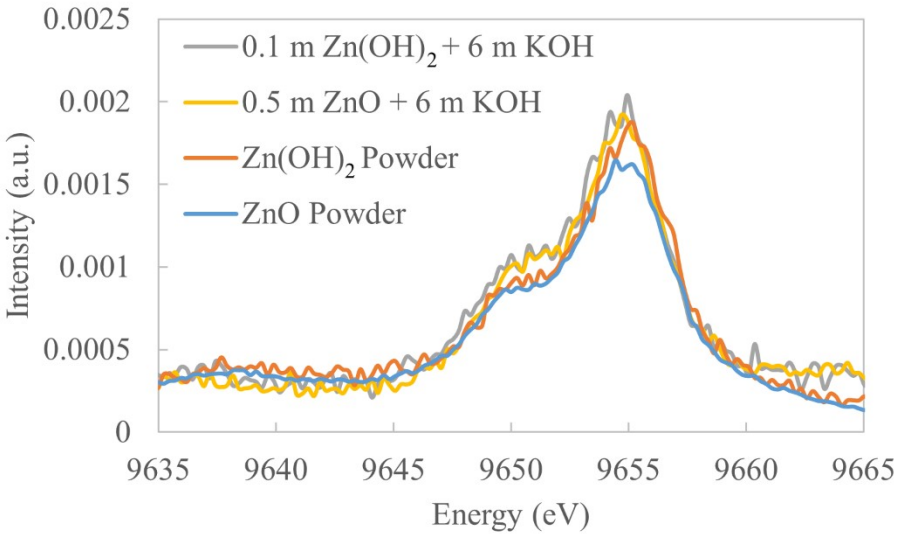

Figure SI-5: VTC-XES spectra of various Zn-species with O as the first neighbor.

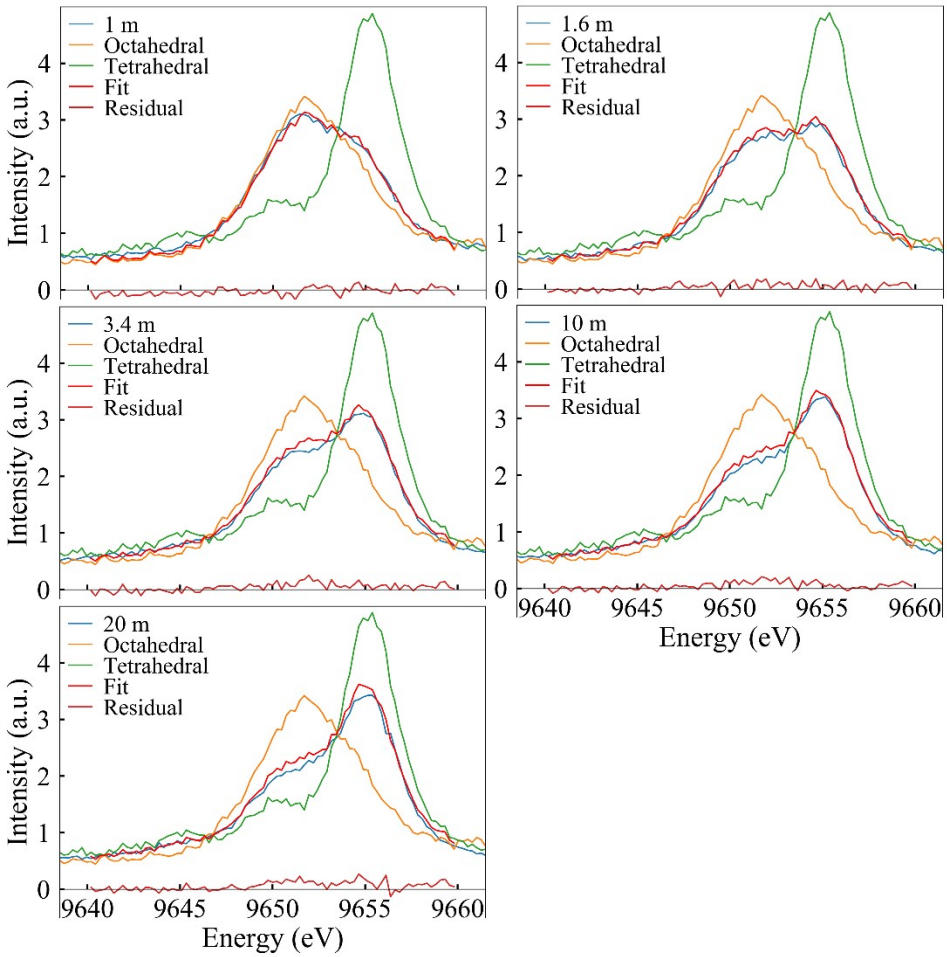

Figure SI-6: LCA fits along with residuals and end point spectra for the $ZnCl_2$ concentration series.

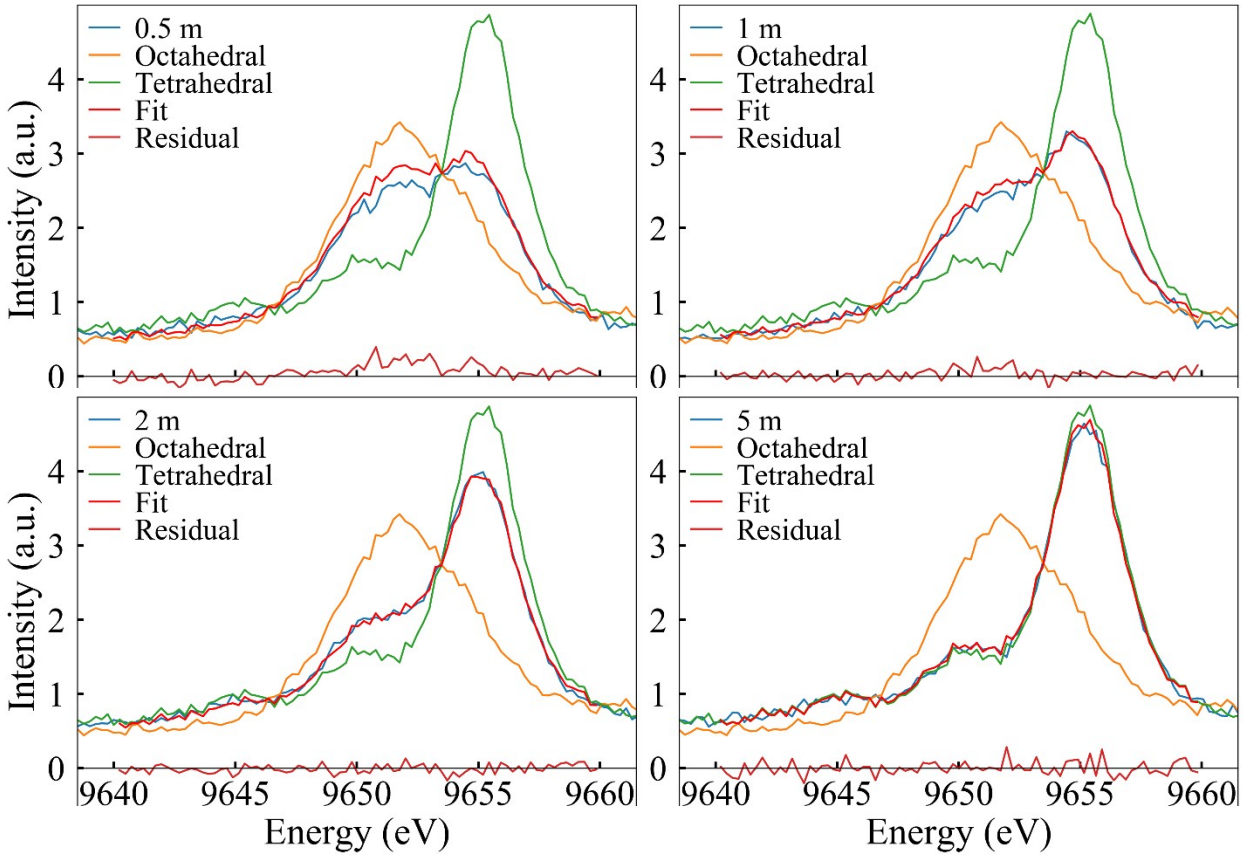

Figure SI-7: LCA fits along with residuals and end point spectra for the samples with composition 1 m $ZnCl_2$ + *x* m NaCl (*x* given in legend).

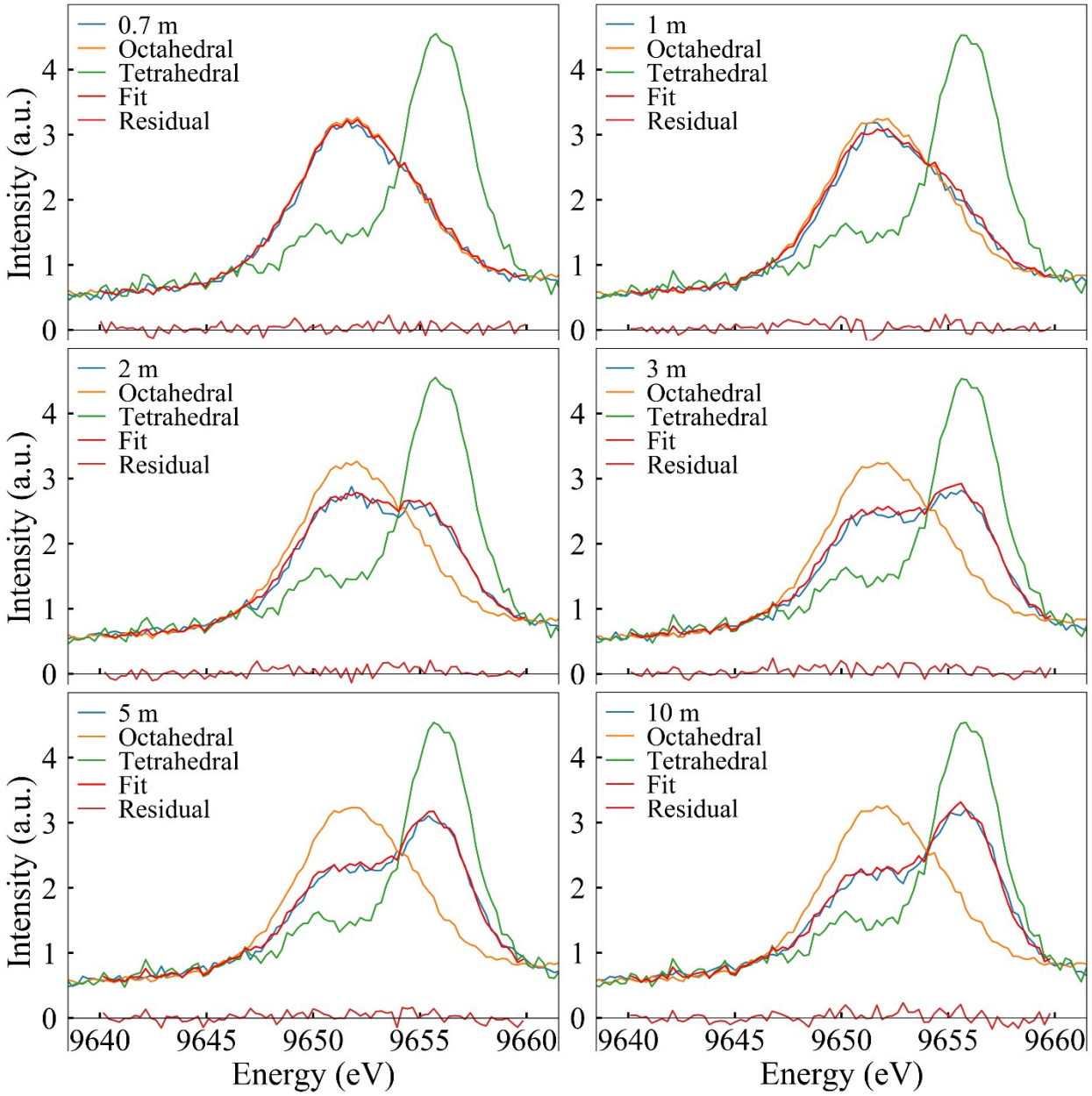

Figure SI-8: LCA fits along with residuals and end point spectra for the $ZnBr_2$ concentration series.

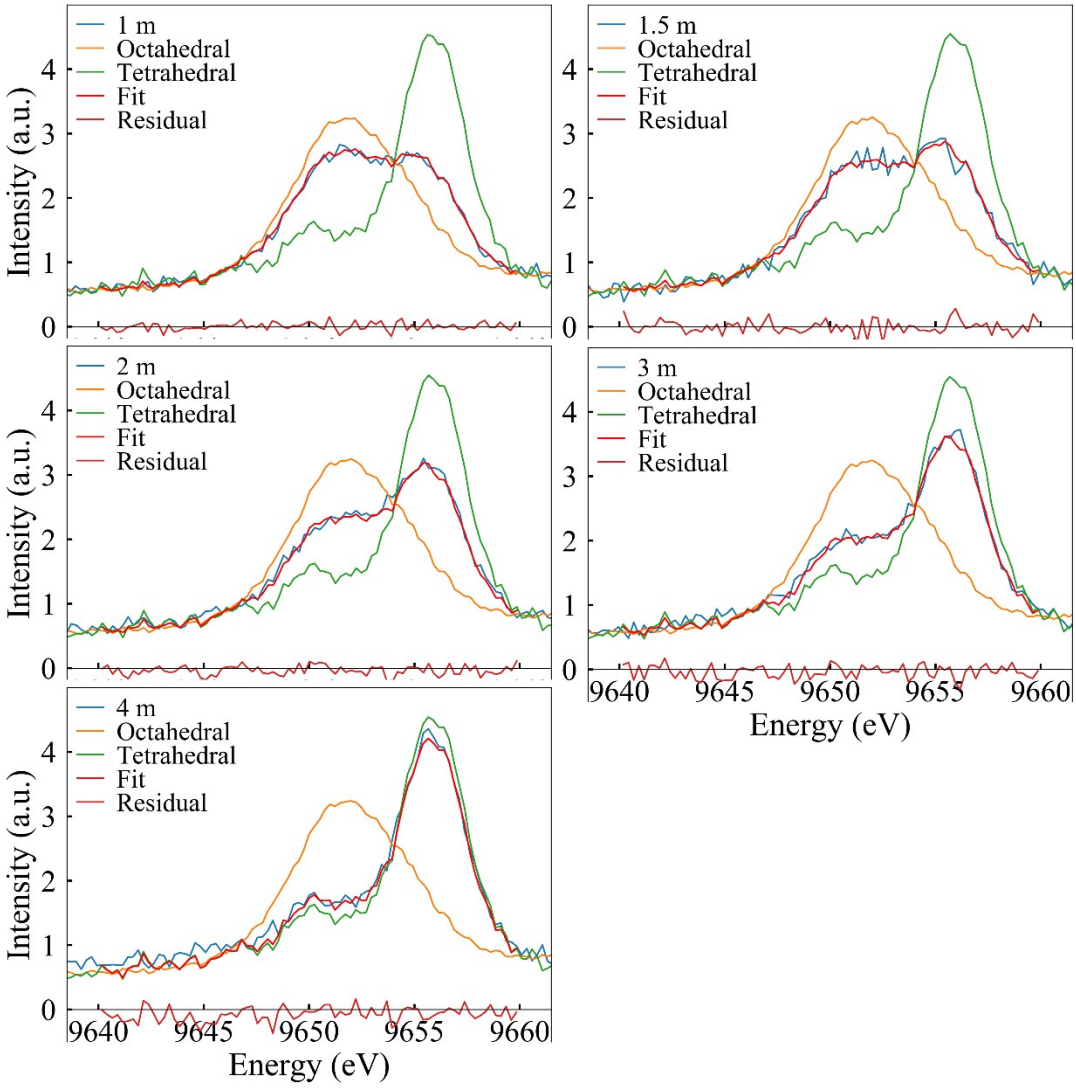

Figure SI-9: LCA fits along with residuals and end point spectra for the samples with composition 1 m $ZnBr_2$ + *x* m LiBr (*x* given in legend).

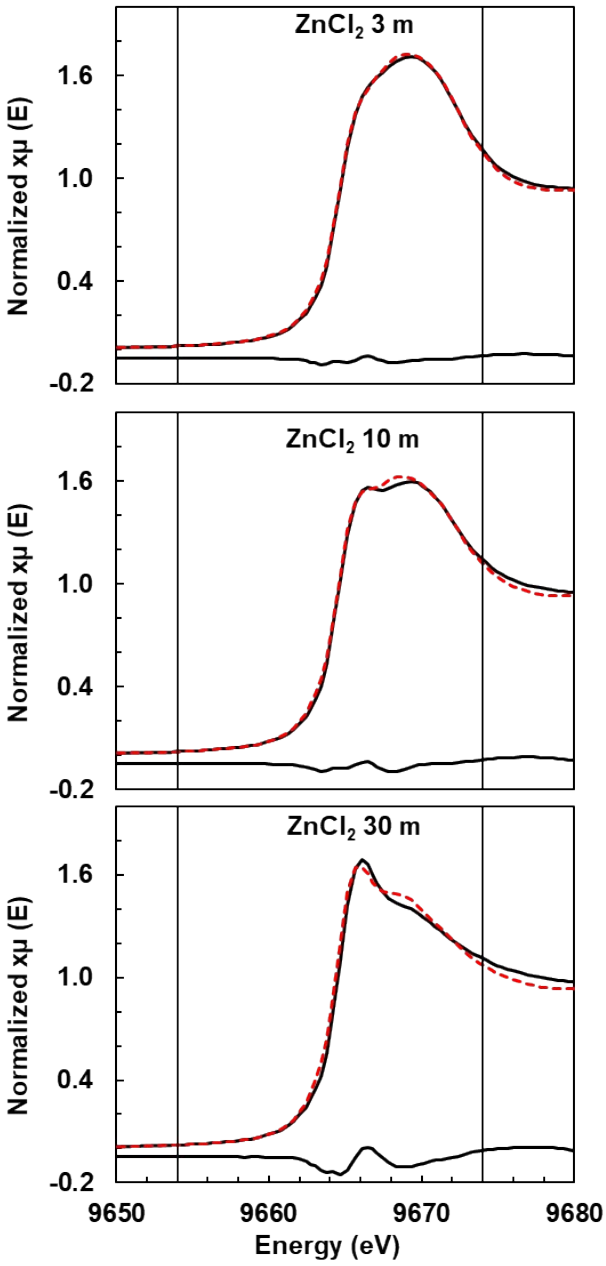
ZnCl2 3 m
ZnCl2 10 m
ZnCl2 30 m
Normalized xμ (E)
1.6
1.0
0.4
-0.2
9650
9660
9670
9680
Energy (eV)

Figure SI-10: Selected LCA fits and experimental XANES data with residual for $ZnCl_2$ concentration series.

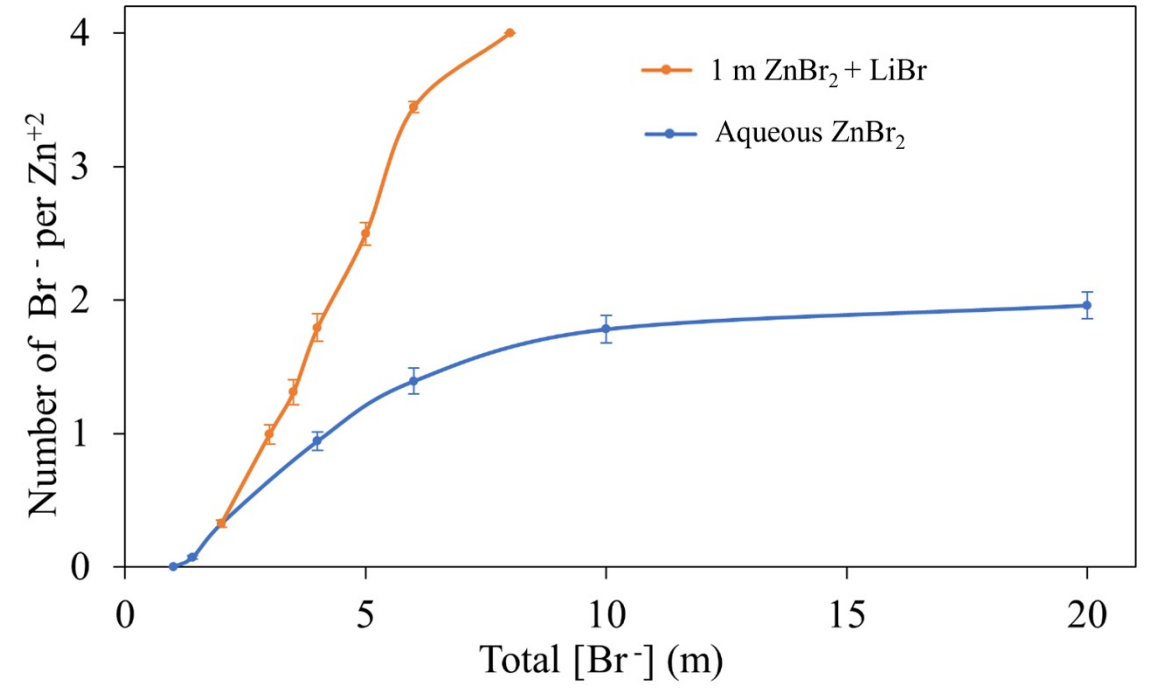

Figure SI-11: Average number of Br^- coordinated with Zn^{+2} in the solution as a function of the total Br^- concentration for pure $ZnBr_2$ concentration series and added salt series.

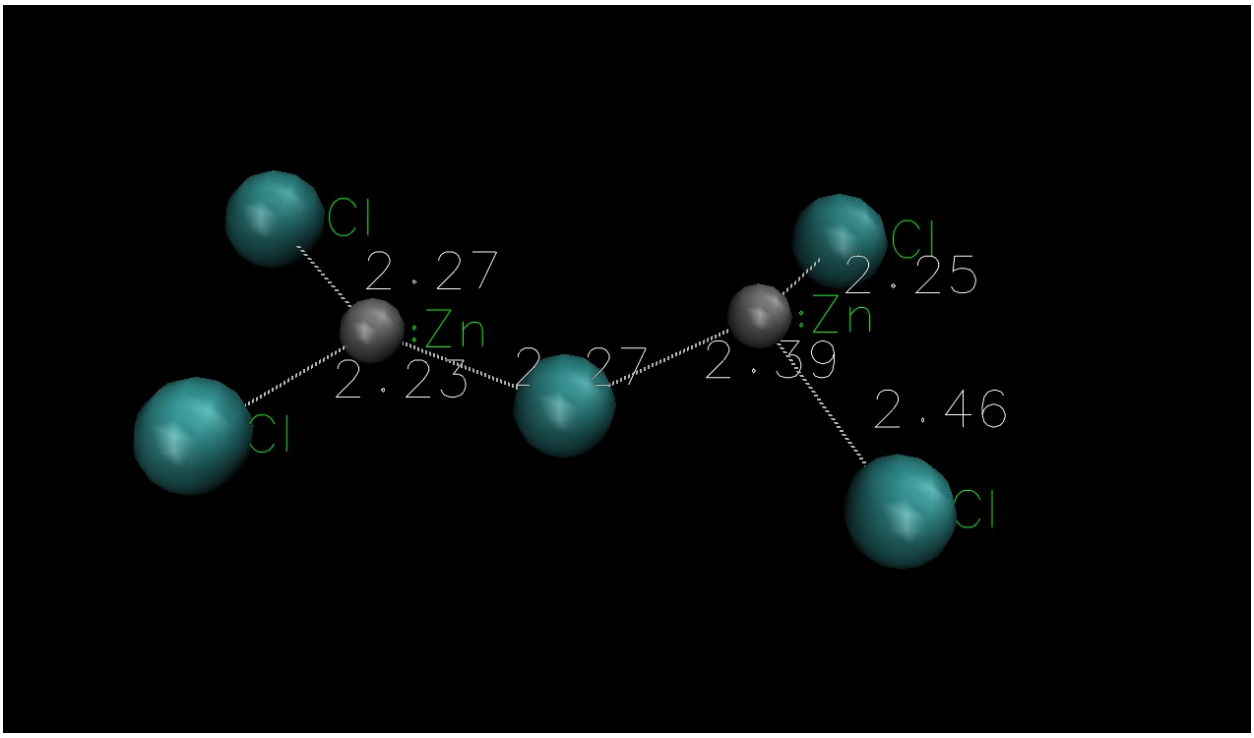

Figure SI-12: MC derived $Zn_2Cl_3^{1-}$ dimer (with bridging Cl) structure. The numerical values are bond lengths in Angstroms.

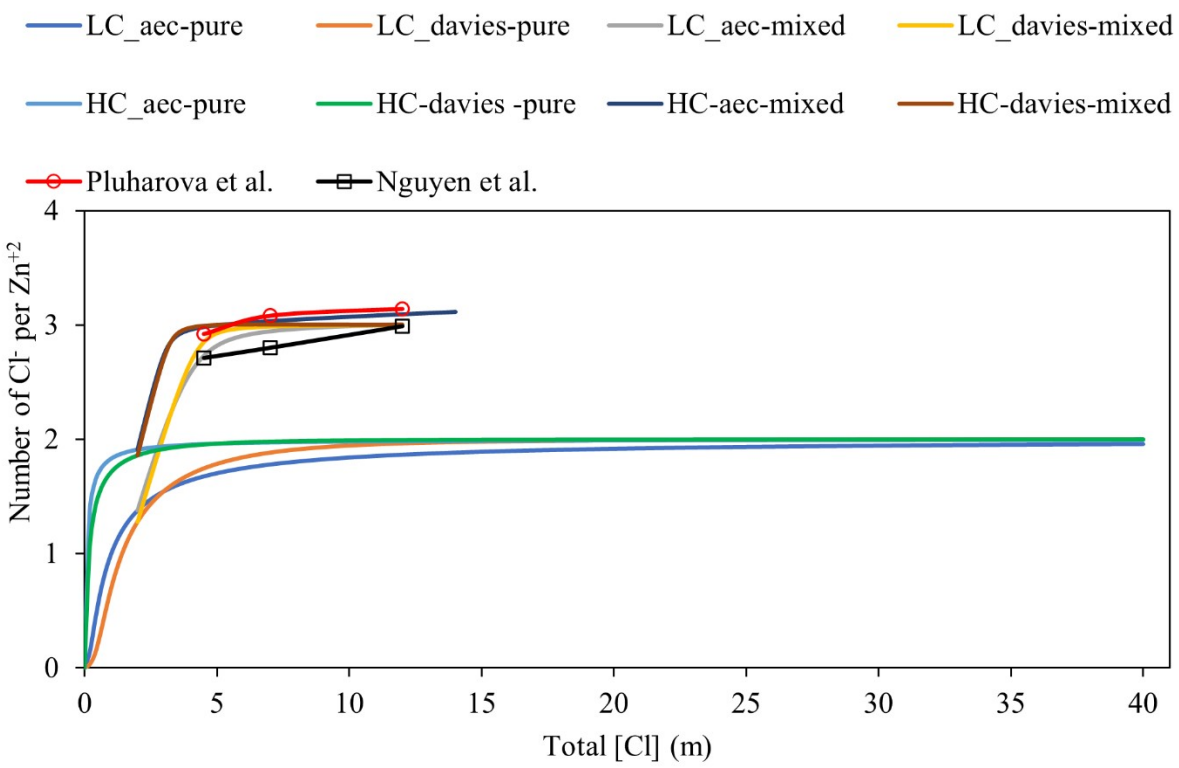

Figure SI-13: Average chloride coordination number per zinc as a function of total chloride concentration for pure and mixed salt solutions derived from various theoretical methods as indicated in the legend. In the legend: LC – low concentration, HC – high concentration, aec – activities are assumed to equal concentrations, Davies – indicates that activity corrections were calculated using the Davies equation, pure – is pure $ZnCl_2$ solutions and mixed - is 1 m $ZnCl_2$ + a variable amount of NaCl. Pluharova et al. is Ref. 53 and Nguyen et al. is Ref. 54 in the manuscript.

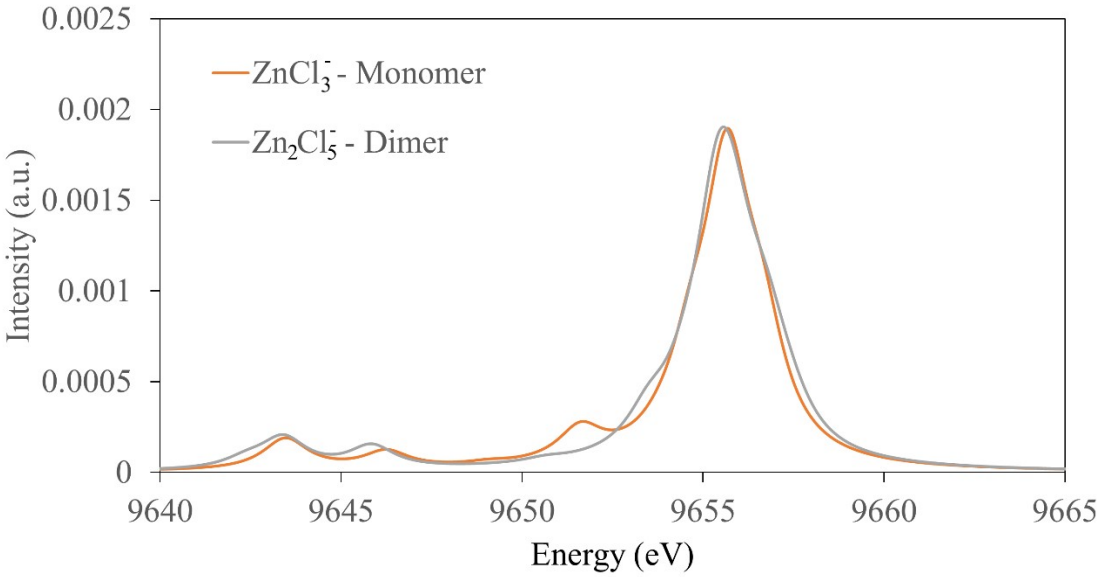

Figure SI-14: TDDFT calculated VTC-XES spectra of dimer $Zn_2Cl_5^-$ and monomer $ZnCl_3^-$.

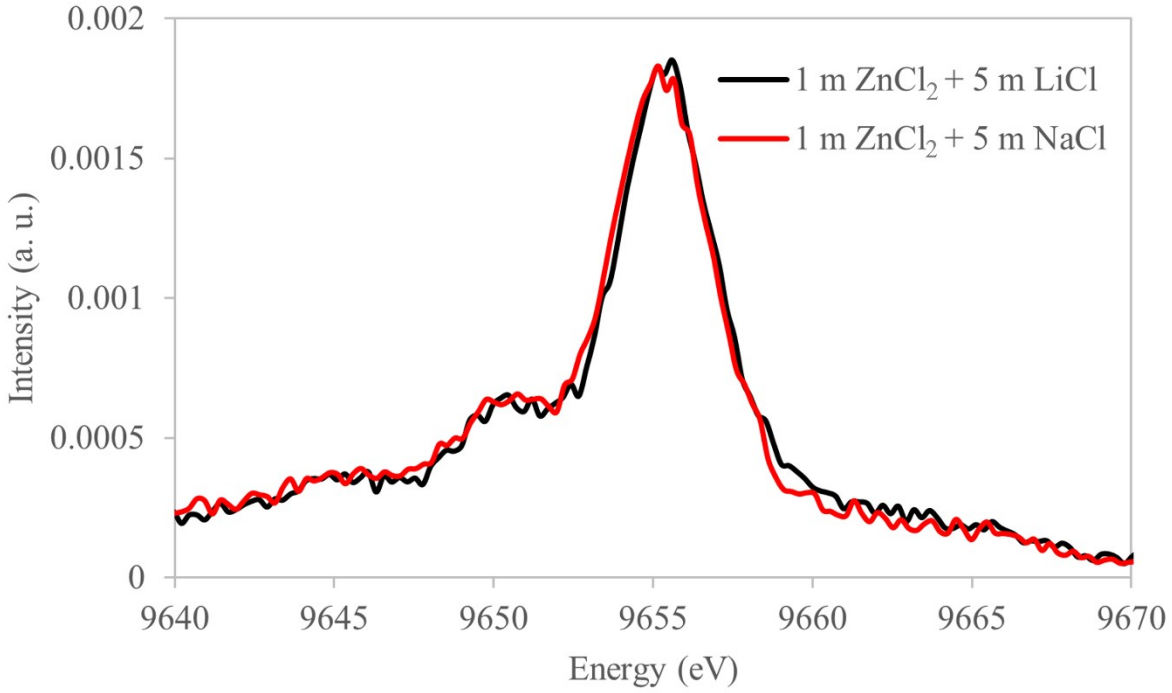

Figure SI-15: Identical experimental VTC-XES spectra for 1 molal $ZnCl_2$ aqueous solutions with added NaCl and LiCl confirming the null effects of the additional cation on the VTC-XES spectra of the Zn-complex.

19. Details of the N_{Cl} calculation

A physical admixture of local environments results in a similarly weighted VTC-XES spectrum:

$$I(E) = \sum_{x=0}^{4} n_x I_x(E) \quad . \qquad (1)$$

where n_x is the fractional contribution of the species with *x* Cl ligands ($\sum n_x = 1$) and $I_x(E)$ is the mole-normalized VTC-XES spectrum for, again, the species with *x* Cl ligands. If the spectra for intermediate moieties are (even approximately) linearly dependent on the endpoint spectra, we would have

$$I_x(E) = (1 - f_x) I_0(E) + f_x I_4(E) . \qquad (2)$$

where f_x is the fraction of tetrahedral weight in $I_x(E)$. While we cannot prepare pure samples of the intermediate moieties to test the validity of Eq. 2, we do find that the TDDFT predicted spectra for the intermediate moieties are indeed very nearly linearly dependent on the endpoint octahedral and nominally tetrahedral fully chlorinated spectra, and furthermore that the linear dependence is quite smooth in *x* (see Table SI-3 for the linear decomposition of calculated intermediate moiety spectra onto the endpoint configurations). The latter detail has a subtle, but very useful consequence: In the idealized smoothly varying case where $f_x = x/4$, Eq. 1 simplifies to a one-parameter expression in terms of the average number of Cl ligands, N_{Cl}, without any ability to infer specific n_x, i.e.,

$$I(E) = \frac{4 - N_{Cl}}{4} I_0(E) + \frac{N_{Cl}}{4} I_4(E) . \qquad (3)$$

If f_x deviates only modestly from $x/4$, as is the case here, then a numerical survey of Eq. 1, constrained by Eq. 2, over the physically allowed solutions to n_x will effectively correct Eq. 3 and find a physically allowed range of values for N_{Cl}.

For the calculation of N_{Cl}, the values for the fractional contribution of intermediate moieties (n_x in equation 1 above) were varied over the range of (+/-) 0.05 around the values obtained from the fitting of calculated VTC-XES spectra (see Table SI-3). The permissible fractions of all intermediate moieties present in each spectrum were allowed to fluctuate anywhere between 0 and 1, such that the mole fraction sum is conserved at unity. The average of all the values obtained for N_{Cl} was then reported with an error bar of one standard deviation (Fig. 6 in the article).

20. Ancillary information about the CMD force field.

The force field was used without modification from some of our prior work (Rampal et al., 2021, Ref. 30 in manuscript). The force field was refined to reproduce the neutron diffraction with isotopic substitution experiments on 4.5 m $ZnCl_2$ solutions. In this method, the differences in the structure factors is measured of two matched solutions in "null" water (with zero coherent scattering from hydrogen) that differ only in the isotope of chloride in the solutions. The Fourier transform of that difference structure factor reveals the atomic-scale Pair Distribution Function (PDF) with respect to chloride. After formal charge models were found to overestimate the extent of solution structuring, an electronic continuum correction method was applied, specifically the force field was adapted from prior work (Duboue-Dijon et al., 2018, Ref. 35 in manuscript; itself developed from total scattering PDF of null water $ZnCl_2$ solutions) to reproduce measured NDIS data more precisely. The parameters to which this force field was tuned reflects

the ion clustering of the solutions specifically, hence the excellent agreement with the XES data in pure $ZnCl_2$ solutions measured here. However, in review, the question was raised about how this force field reproduces other thermodynamic properties of the system, in particular the hydration free energies of the aqueous ions. To examine this, we calculated an average potential energy difference for the hydrated aqueous ions and water, and applied a correction for the ECC's model's lack of formal charges (Döpke et al., 2020, (Ref. 1)). These give hydration free energies of zinc and chloride as -1904 and -374 kJ/mol, respectively. The experimental estimates are -1975 and -344 kJ/mol, for Zn^{2+} and Cl^-, respectively (Marcus, 2015, (Ref. 2)). Considering the force field was not tuned to reproduce the hydration free energy specifically, the agreement is acceptable. While improvement could be made for zinc especially, we stress that this force field is designed to reproduce the atomic-scale solution structure, especially the extent of ion clustering. Previous work has shown that for classical models, improving agreement with one set of calibration data often leads to a degradation in the agreement of others (Biriukov et al., 2022, Ref. 68 in manuscript). Thus, a precise match for hydration free energy will likely lead to a degradation of the ability to model ion clustering.

References:

1. Döpke, M. F.; Moultos, O. A.; Hartkamp, R.; On the transferability of ion parameters to the TIP4P/2005 water model using molecular dynamics simulations. J. Chem. Phys. 152, 024501, 2020.
2. Marcus, Y.; Ions in Solution and their Solvation. John Wiley & Sons, Incorp. Hoboken, NJ, 2015